KAOLINITE/MONTMORILLONITE RESEMBLES BEIDELLITE

J. Cuadros,[1] A. Delgado,[1] A. Cardenete,[2] E. Reyes,[1] and J. Linares[1]

[1] U.E.I. Fisicoquímica y Geoquímica Mineral, Estación Experimental del Zaidín (C.S.I.C.)
Profesor Albareda 1, 18008 Granada, Spain

[2] Departamento de Química Física, Facultad de Ciencias
Universidad de Granada, Campus Universitario de Fuentenueva, 18001 Granada, Spain

Abstract—A number of smectitic samples from Almería (SE Spain) were studied by chemical analysis, DTA, TG, XRD (oriented aggregates with ethylene glycol treatment and Greene-Kelly test), FTIR and MAS NMR. Chemically they resembled a beidellite-montmorillonite series, displaying DTA/TG characteristics already quoted in the literature in beidellite descriptions. They did not swell after the Greene-Kelly test, as it has also been reported for some beidellites. Nevertheless XRD of the oriented, glycolated samples, FTIR, MAS NMR and revision of the chemical analysis demonstrated that they were mixed-layered kaolinite/montmorillonite. It is possible that some of the reported beidellites in the literature are kaolinite/montmorillonite. Beidellite characterization must be supported by several different techniques.

Key Words—Beidellite, Greene-Kelly test, Kaolinite/montmorillonite.

INTRODUCTION

Beidellite is chemically defined as a dioctahedral smectite with low iron content [less than 0.5 on the basis of $O_{20}(OH)_4$] whose negative charge is provided mainly by Al for Si substitution in its tetrahedral sheet. Montmorillonite, which is much more abundant, presents a charge arising mainly from the substitution of Mg for Al in the octahedral sheet (Newman and Brown, 1987; Güven, 1991).

Beidellite is generally characterized by means of chemical analysis which is in principle easy if there is certainty about the fact that one has monomineralic samples. Another important method used to characterize beidellite, distinguishing it from montmorillonite, is the Greene-Kelly test (Greene-Kelly, 1952). This method is used by many researchers with apparent success, but it has been emphasized that it is not always determinative. Some smectites chemically characterized as beidellites behaved as montmorillonites in the Greene-Kelly test (Wilson, 1987; Brindley and Lemaitre, 1987; Bystrom-Brusewitz, 1975; Malla and Douglas, 1987).

DTA has also tentatively been used to differentiate beidellite from montmorillonite with contrasting results. Some authors found no difference in the minerals' thermal behaviour (Brindley and Lemaitre, 1987), others found differences in the endothermic peak corresponding to the loss of interlayer water (Paterson and Swaffield, 1987). A third group pointed out that the dehydroxylation endothermic peak appears in the 500°–600°C range for beidellite and 600°–700°C for montmorillonite (Mackenzie, 1970; Borchardt, 1977). In agreement with the latter group, a study of SCIFAX DTA Data Index (1962) file shows that in most cases beidellite exhibits the dehydroxylation peak in the lower range of temperature, and montmorillonite in the upper one. In many cases smectites present two dehydroxylation peaks.

Schultz (1969) found by means of TG that beidellites had in many cases a dehydroxylation weight loss greater than the ideal one, that is, the one calculated on the basis of the structural formula. Chemical analyses of beidellites in which the amount of structural water is displayed are rare in the literature. Nevertheless we have found that many beidellites have higher structural water contents than montmorillonites.

We present here the results of a study of a number of smectitic samples which were initially interpreted as a montmorillonite-beidellite series on the basis of chemical analysis and powder XRD. Subsequent careful XRD study of the glycolated samples associated with FTIR, DTA/TG and revision of chemical analysis showed them to be kaolinite/montmorillonite mixed-layer. MAS NMR of three of the samples confirmed it.

MATERIALS AND METHODS

We studied 55 samples from the deposit of "Los Trancos," in Almería (SE Spain). They are smectites developed in response to hydrothermal alteration of a very homogeneous volcanic tuff of acid composition (the volcanic tuff could be observed in some un-altered zones). The volcanic events that produce the tuff occurred during the Middle-Upper Tortonian. The altered bulk rock was crushed and finely ground in an agate mortar. XRD analysis of the resulting powder showed a high smectite content of more than 90% in weight and the absence of trioctahedral smectites. Smectites were sampled from the deposit surface (LT samples) and at depths increasing to 50 m below the surface (T samples are shallower than TR ones). Only

that fraction smaller than 2 μm was used. It was separated by dispersion in water and sedimentation. The smectites were not further treated.

Chemical analyses of LT samples were taken from Reyes *et al.* (1978). Those for T samples were carried out by wet analysis. TR samples were analysed by XRF using an X-ray fluorescence spectrometer PW 1404 with Cr-Au dual anode tube and LiF 200, LiF 220, Ge, PE, and Px1 analyser crystals. Samples were diluted (1:10) in $Li_2B_4O_7$ and fused. CEC was determined by saturation of samples with NH_4^+ (ammonium acetate) at pH 7, later displacement of NH_4^+ with Na (NaCl), also at pH 7, and NH_4^+ analysis by Kjeldahl's method. The detailed procedure is described by the Soil Conservation Service (1972). Exchangeable cations were analysed from the solutions after NH_4^+ saturation. The amorphous materials were identified chemically. Fe-phases were extracted using the dithionite-citrate-bicarbonate method. Al- and Si-phases were extracted with Na_2CO_3. Subsequent determination of Fe, Al and Si was carried out by wet analysis.

For the Greene-Kelly test, samples were Li exchanged by dispersion in 3 M LiCl. Exchanged samples were washed until the test for Cl^- presence by addition of $AgNO_3$ was negative. The oriented aggregates were prepared by placing some drops of the dispersed samples on glass slides and leaving them to dry. The oriented aggregates were heated at 280°C for 24 hours. Afterwards, they were placed in a heater at 100°C in a glycerol atmosphere for 24 hours. Finally, they were X-rayed in a Philips PW 1710/00 diffractometer with CuKα radiation, graphite monochromator and automatic slit (scan speed 0.2 °2θ/s and counting time 0.4 s). Nine selected samples were also studied by means of XRD after glycolation. They were analysed without previous cation exchange. They were oriented in the way indicated above, heated at 60°C in ethylene-glycol atmosphere for 24 hours and X-rayed. Data were recorded in diskette and computer-analysed (POLVO program).

DTA and TG curves were simultaneously obtained at a heating rate of 10°C/min in air, with alumina as reference in alumina sample holders. Sample weights were between 30–35 mg. They were run in a NETZSCH Simultaneous Thermal Analysis STA 409 EP with a Temperature Programmer 410 controlled by computer. Output data were recorded in diskettes. The controlling program is supplied with a number of facilities for data-processing (the specific facilities of interest for the present analysis are the quantification of DTA peak areas and of percentages of mass loss during some selected stages of the TG diagrams).

IR spectra were obtained in a FTIR spectrometer NICOLET 20SXB working with 2 cm^{-1} resolution. The samples were diluted 1:100 in KBr. The bands were decomposed by means of a mathematic algorithm which calculated the components fitting the spectrum, together with their respective areas. The standard deviation of the calculated spectra with respect to the original ones was always lower than 1.2%.

MAS NMR analysis was carried out with a Bruker AMX300 spectrometer. The ^{27}Al spectra were recorded at 78.23 MHz using a pulse width of 4 μs, a spectral width of 50 kHz, a recycle delay of 0.3 s, 6000 scans and 10 Hz Gaussian line broadening. The samples were rotated at a speed of 3.5 kHz. Chemical shifts are reported in ppm from 0.1 M $[Al(H_2O)_6]^{+3}$.

EXPERIMENTAL RESULTS

Chemical data

Chemical analysis of some of our samples are shown in Table 1. They are representative of all of them, as they cover the whole range of chemical composition. They have been selected because their analysis by other techniques are shown below, and it is interesting to have the chemical data for comparison. The samples were initially interpreted as purely smectitic on the grounds of powder XRD. For this reason the corresponding structural formulae were calculated. This was achieved using the method proposed by Marshall (1949), with the appropriate corrections for exchangeable Mg and amorphous phases. In Table 1 are also shown the corresponding structural formulae. In it, the tetrahedral charge corresponds to Al for Si substitution in the tetrahedral sheet. The total charge is obtained by measuring the CEC. The octahedral charge is the difference between total and tetrahedral charge. The main feature of these results is that they could represent a reasonable montmorillonite-beidellite series.

DTA/TG data

Six DTA and TG diagrams are shown in Figure 1. Two dehydroxylation peaks and their corresponding weight loss are observed, around 510° and 650°C. A relation between the shape of DTA/TG diagrams and the chemical composition of the samples appears. The peak at lower temperature increases, with a corresponding decrease of the peak at higher temperature, as alumina content in the sample does. The peak at higher temperature is always present, but it is sometimes reduced to a shoulder. This relation was quantified measuring and comparing the two peak areas. The areas were calculated (by means of the thermal analyser software) tracing a straight line from the onset to the end of each peak and measuring the area under the line. In many samples the end of the peak at lower temperature could not be differentiated from the onset of the peak at higher temperature. In these cases the point of lower peak end was also taken as the higher peak onset. The percentages of dehydroxylation peak area at 650°C versus total dehydroxylation area are shown in Figure 1.

The correlation between the Al_2O_3 percentage in the chemical analysis and the area percentage of the peak

Table 1.   A. Chemical analysis of samples. "n.d." stands for not determined. B. C.E.C., exchangeable cations and amorphous phases of samples. C. Structural formulae of samples, on the basis of $O_{20}(OH)_4$, considering them as pure smectites. They resemble a montmorillonite-beidellite series.

A

Sample	SiO_2	Al_2O_3	Fe_2O_3	TiO_2	CaO	MgO	Na_2O	K_2O	H_2O^+	%
T-20	54.96	21.75	3.90	n.d.	1.12	5.02	0.73	0.18	12.40	100.06
LT-2	54.85	25.08	2.14	n.d.	1.88	3.78	1.32	0.34	10.34	99.73
LT-3	57.18	23.10	1.35	n.d.	1.71	4.64	1.38	0.25	9.34	98.95
LT-9/3	58.70	22.29	1.13	n.d.	1.59	5.01	1.81	0.28	8.89	99.70
LT-10/1	54.98	24.58	1.60	n.d.	2.07	3.78	1.36	0.30	10.63	99.30
TR-1	61.30	21.50	2.53	0.14	1.01	4.66	0.22	0.14	8.36	100.01
TR-4	60.04	21.12	1.20	0.27	1.27	6.33	1.37	0.20	9.76	101.56
TR-115	58.40	23.72	2.71	0.18	1.20	4.39	0.20	0.09	9.42	100.31
TR-117	56.55	24.66	3.00	0.21	1.05	3.75	0.09	0.08	10.27	99.66
TR-119	59.56	23.39	2.67	0.19	1.23	4.34	0.15	0.09	9.51	101.13
TR-121	57.09	24.09	2.91	0.20	1.06	3.66	0.10	0.11	10.47	99.69
TR-125	58.80	24.11	2.68	0.18	1.14	4.48	0.14	0.13	9.60	101.26
TR-146	61.59	18.23	2.67	0.20	1.37	6.17	0.12	0.26	9.15	99.76

B

Sample	C.E.C.	Exchangeable cations (meq/100 g)				Amorphous phases (%)		
		Ca^{2+}	Mg^{2+}	Na^+	K^+	SiO_2	Al_2O_3	Fe_2O_3
T-20	82	14	51	17	1	0.42	0.12	0.07
LT-2	94	27	54	23	1	0.69	<0.05	<0.05
LT-3	104	46	55	27	1	0.68	<0.05	<0.05
LT-9/3	107	31	57	14	0	0.87	<0.05	<0.05
LT-10/1	81	27	46	7	1	0.61	<0.05	<0.05
TR-1	118	38	70	13	2	0.90	<0.05	<0.05
TR-4	110	40	63	13	2	1.22	0.10	0.28
TR-115	108	40	63	11	1	0.92	0.34	0.18
TR-117	90	35	54	9	1	0.88	0.25	0.20
TR-119	108	42	61	9	1	0.72	0.06	0.17
TR-121	90	36	52	8	1	0.88	0.47	0.17
TR-125	99	34	62	9	1	0.86	0.28	0.19
TR-146	116	48	61	8	3	1.01	0.20	0.44

C

Sample	[4]Si	[4]Al	[6]Al	[6]Fe	[6]Mg	[6]SUM	Total charge	Oct. charge
T-20	7.50	0.50	3.00	0.40	0.81	4.20	0.70	0.20
LT-2	7.35	0.65	3.36	0.22	0.56	4.14	0.78	0.13
LT-3	7.58	0.42	3.24	0.14	0.72	4.10	0.86	0.44
LT-9/3	7.68	0.32	3.18	0.11	0.79	4.08	0.87	0.56
LT-10/1	7.44	0.56	3.40	0.16	0.60	4.17	0.67	0.10
TR-1	7.82	0.18	3.09	0.24	0.63	3.96	0.92	0.74
TR-4	7.75	0.25	3.02	0.11	0.99	4.12	0.87	0.63
TR-115	7.58	0.42	3.21	0.24	0.61	4.06	0.86	0.43
TR-117	7.46	0.54	3.31	0.28	0.53	4.12	0.72	0.18
TR-119	7.63	0.37	3.19	0.25	0.60	4.04	0.84	0.47
TR-121	7.56	0.44	3.31	0.25	0.52	4.08	0.73	0.29
TR-125	7.56	0.44	3.23	0.24	0.63	4.10	0.78	0.34
TR-146	7.96	0.04	2.80	0.25	0.98	4.03	0.93	0.89

at 650°C ($\%M_{DTA}$) is shown in Figure 2. The amounts of amorphous alumina detected by chemical analysis (Table 1) were subtracted from the total alumina contents prior to achieve the correlation. Although there is some scattering, the relation between alumina content and dehydroxylation behaviour is apparent. Higher amounts of alumina correspond to larger dehydroxylation peak areas at the lower temperature. This is consistent with many reported data in which beidellites exhibit dehydroxylation temperatures lower than those

found in montmorillonites (SCIFAX DTA Data Index, 1962).

The amounts of hydroxyl loss were also measured by means of TG and correlated with the sample alumina contents. The measuring of the amount of hydroxyl loss was achieved as follows. The dehydroxylation stage was delimited by the change of slope of the TG diagram together with the onset and end of the DTA peaks. In this way the true dehydroxylation stage was separated from the continuum mass loss which
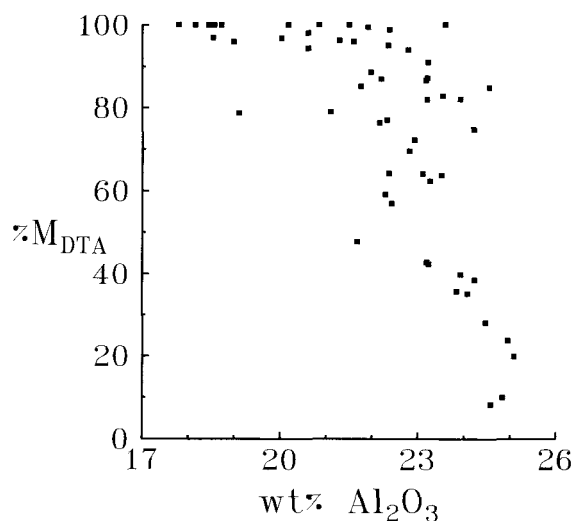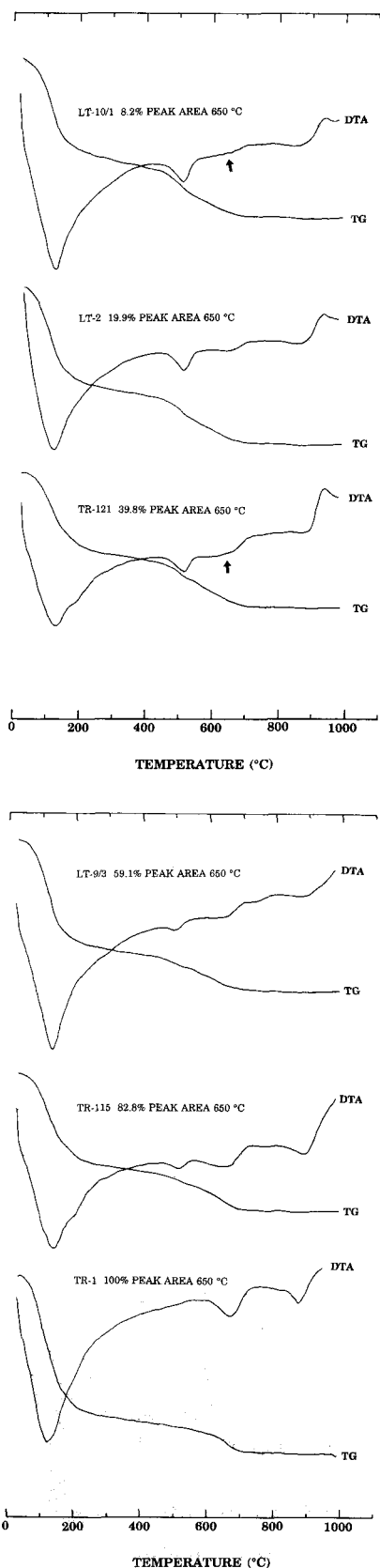
Figure 2. Percentages of dehydroxylation peak area at 650°C versus percentages of alumina content.

occurs between dehydration and dehydroxylation. Finally the percentage of mass loss in the delimited stretch was measured. The results are shown in Figure 3. As alumina content increases the amounts of hydroxyl loss also do.

XRD data

The Greene-Kelly test was carried out to obtain further evidence about the presence of beidellite in our samples. But it yielded negative results in all of them. None of the samples swelled. Diffractograms of four samples are shown in Figure 4. The measured percentage area of their dehydroxylation peaks at 650°C are included. Their chemical analyses can be seen in Table 1. Neither different chemical compositions nor dehydroxylation behaviours of the samples modified the Greene-Kelly test results.

Nine samples covering the whole range of chemical composition ($SiO_2:Al_2O_3$ wt. % ratio) were selected to be glycolated and X-rayed. The diffractograms of four of them are shown in Figure 5. They correspond to the extreme values of $SiO_2:Al_2O_3$ ratio of the nine samples studied and to two intermediate values. In them, $SiO_2:Al_2O_3$ ratio increases from TR-117 to TR-4. The intensities of the (001) reflections are different, although this cannot be shown in Figure 5. Their relative intensities are TR-4: 100, TR-119: 23, TR-121: 18, TR-117: 14.

←

Figure 1. DTA and TG curves of six selected samples showing two dehydroxylation stages. Arrows indicate the position of the higher DTA dehydroxylation peak in two samples in which it is reduced to a shoulder. The corresponding chemical data can be seen in Table 1.
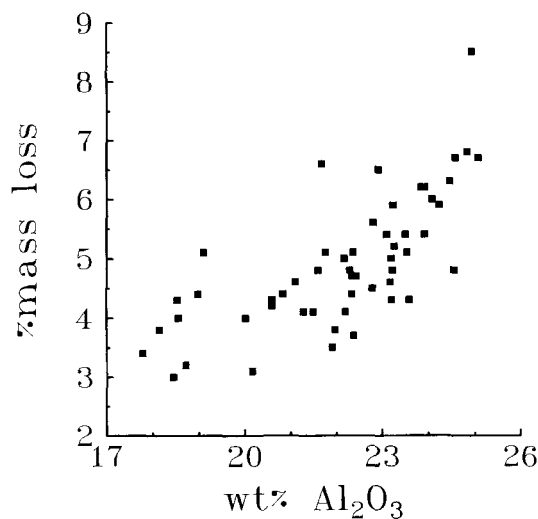
Figure 3. Percentages of mass loss in dehydroxylation versus percentages of alumina content of the samples.
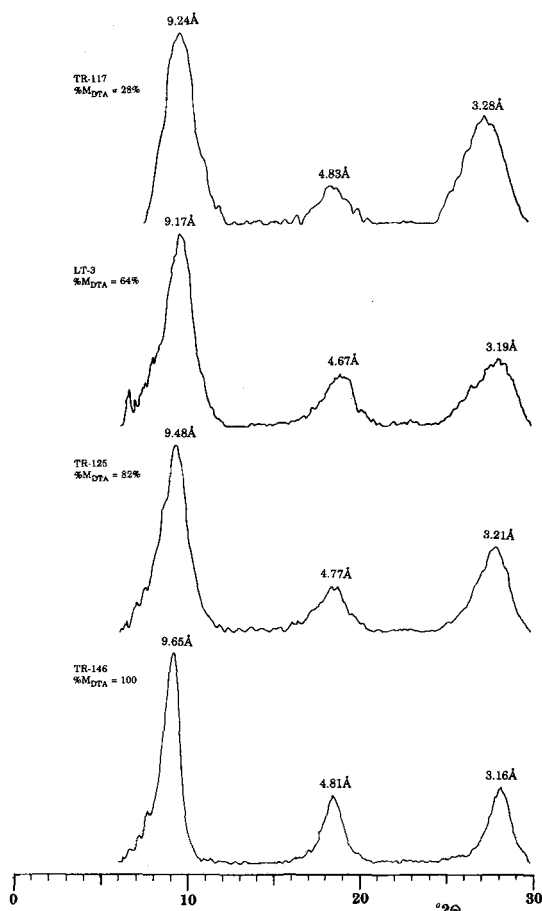

Figure 4. XRD diagrams of four Li-treated samples with preferred orientation and glycerol treatment. The background has been subtracted. Although the samples have different chemical compositions and dehydroxylation behaviour, none of them presents swelling.
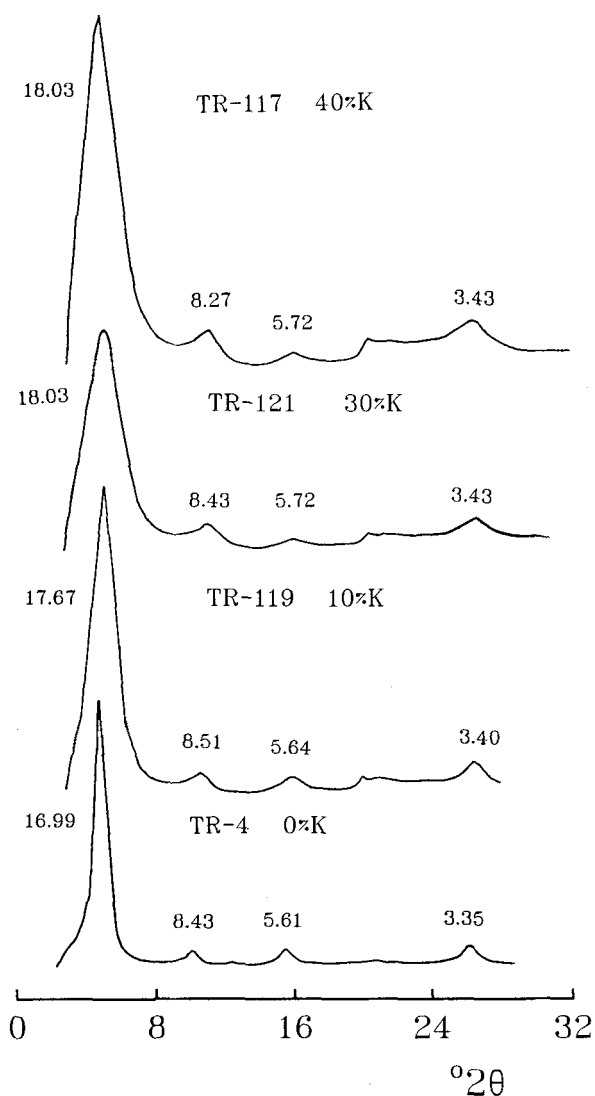

Figure 5. XRD diagrams of four oriented and glycolated samples. Peak labels are in Å. Kaolinite percentages are shown (see text).

In the TR-119, TR-121 and TR-117 samples the maxima positions are irrational. This fact, and the decreasing intensity of the (001) reflections, suggest the presence of interstratification. In fact, comparison with Table 7.5 from Moore and Reynolds (1989) shows them to be R = 0 kaolinite/montmorillonite mixed layer. In Moore and Reynolds' table the positions of 001/002 and 002/005 maxima in the diffractogram of K/M random interstratificates are related with layer percentage of the two components. The difference of °2θ for the two maxima considered was used to determine the layer composition rather than the absolute value of their positions. In this way, possible difficulties arising from different swelling of the samples are avoided. The
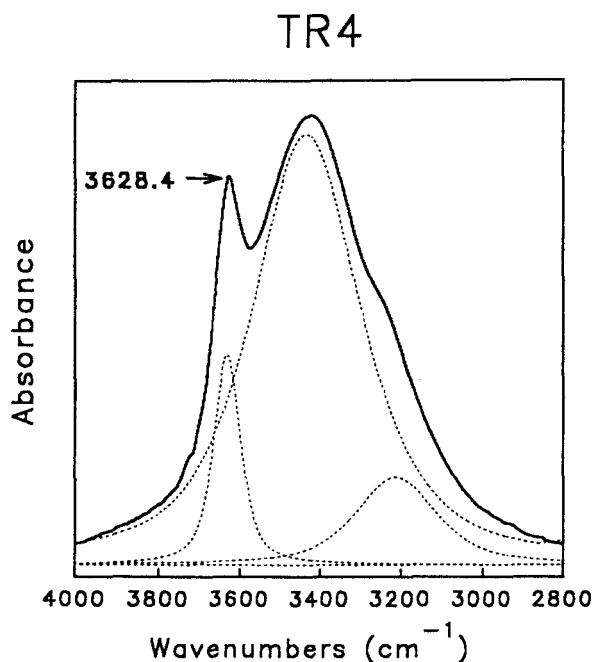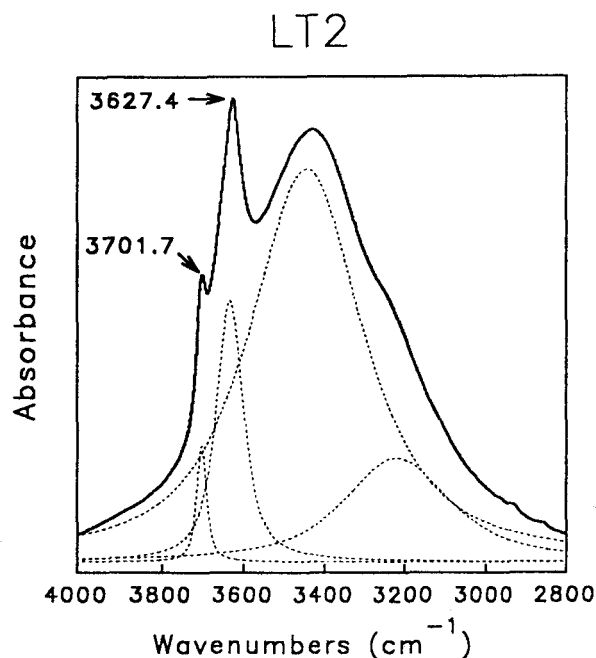
LT2

TR4

Figure 6. FTIR spectra in the hydroxyl stretching region for a sample with high (TR-4) and low (LT-2) $SiO_2:Al_2O_3$ ratio. The band at 3701 cm^{-1} is assigned to stretching of outer hydroxyls in kaolinite. The band at 3627 cm^{-1} corresponds to stretching of inner hydroxyls in both kaolinite and smectite. The broad bands correspond to interlayer water. The bands are decomposed for their quantification.
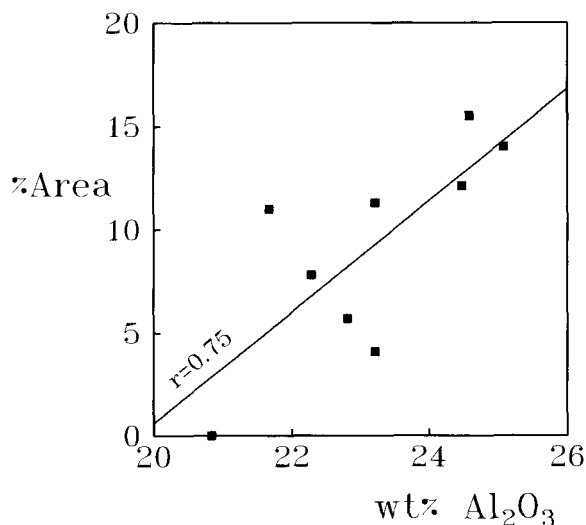

Figure 7. Correlation between percentages of the 3700 cm^{-1} IR band areas and percentages of alumina contents of nine selected samples (see text).

resulting amounts of kaolinite layers are shown in Figure 5.

IR data

The same nine samples which were glycolated and X-rayed were also studied by means of IR spectroscopy. Their spectra are those typical of montmorillonite. Two features are observable. As alumina content in the samples increases, the Al_2OH libration band around 915 cm^{-1} (Farmer, 1974) increases in intensity and the AlOHMg libration band over 840 cm^{-1} (Farmer, 1974) decreases. The second feature is the presence of an hydroxyl stretching band at 3700 cm^{-1} in many samples. This band is assigned to the outer kaolinite hydroxyls (Farmer, 1974; Russel, 1987). Figure 6 shows the hydroxyl stretching zone of two spectra from samples with extreme $SiO_2:Al_2O_3$ ratios within the whole sample set (TR-4 corresponds to the high ratio, LT-2 to the low one).

The areas of the 3700 cm^{-1} band were quantified for each sample and correlated to the Al_2O_3 percentages. For this, the IR bands were decomposed as Figure 6 shows. The areas of both bands at 3627 and 3700 cm^{-1} were added and the area of the 3700 cm^{-1} band was expressed as the percentage of the total area. With this procedure the results of all samples are normalized and become perfectly comparable. Figure 7 shows the correlation. Although the correlation factor is not very high, it can be seen that as the alumina content increases, the area of the 3700 cm^{-1} band also increases.

NMR data

Three samples were analysed by means of MAS NMR. The ^{29}Si spectra are approximately identical,
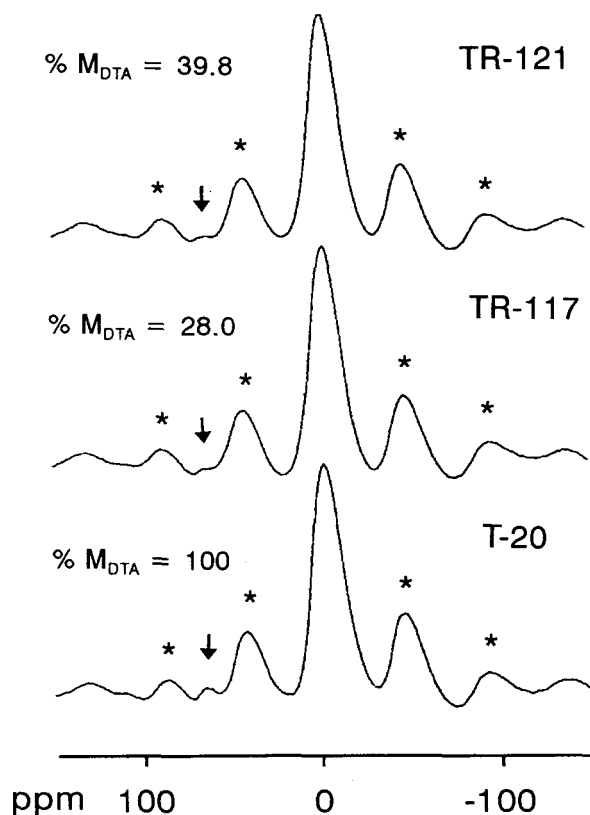
Figure 8. ^{27}Al MAS NMR spectra of three samples. The arrows mark the Al^{IV} bands. The central bands correspond to Al^{VI}, and their spinning side-bands are marked with asterisks. Their corresponding dehydroxylation peak area percentages at 650°C (%M$_{DTA}$) are also shown.

Figure 9. The kaolinite percentage is calculated by means of this plot. The line unites the SiO$_2$:Al$_2$O$_3$ (wt. %) ratios for 0 and 100% kaolinite. The intersection of each ordinate value with the line yields the corresponding kaolinite percentage on the abscissa. There are only eight data points because the values of two of them coincide.

but the ^{27}Al ones show different amounts of tetrahedral Al. Figure 8 shows the NMR spectra. Figure 8 also shows the corresponding percentages of the 650°C dehydroxylation peak areas (%M$_{DTA}$). Their SiO$_2$ and Al$_2$O$_3$ contents can be seen in Table 1.

DISCUSSION

Although the examination of powder XRD and chemical analysis data led to the interpretation of these samples as a montmorillonite-beidellite series, the other techniques permitted to determine the presence of kaolinite, and to characterize them as K/M mixed-layer. Nevertheless, a clue leading to the presence of kaolinite can be seen in the chemical analyses alone, because there is a relation between CEC and alumina content: as the former increases (higher amount of kaolinite) the latter decreases.

The presence of the 3700 cm^{-1} band is diagnostic. As previously quoted, it is assigned to the stretching of outer hydroxyls in kaolinite. Smectites, montmorillonite or beidellite, do not present this band. Moreover, the correlation between alumina content in the samples an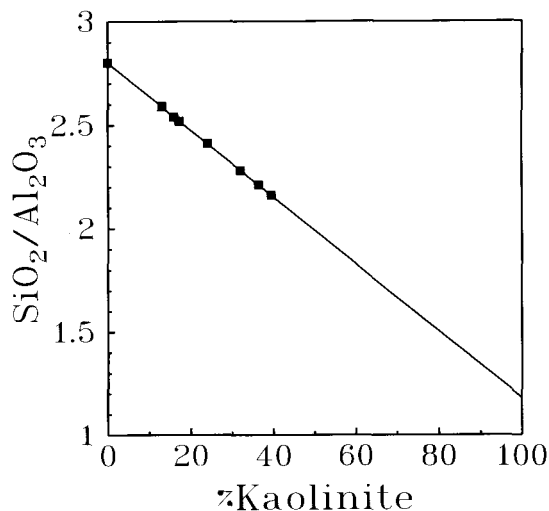d the area of the 3700 cm^{-1} band of Figure 7 is in agreement with the presence of kaolinite. Higher kaolinite contents involve higher alumina contents too. Finally, this interpretation also agrees with the detection of increasing intensities of the Al$_2$OH libration band (915 cm^{-1}) as the alumina content in the samples increases.

TG and DTA data also support the presence of kaolinite. Kaolinite dehydroxylation peak appears in the range 500°–600°C (Paterson and Swaffield, 1987). The peak at lower temperature in the DTA diagram (Figure 1) could correspond to kaolinite, and the higher temperature peak to montmorillonite. It could explain the correlation shown in Figure 2. The area of the high temperature peak decreases as alumina content in the sample increases. Alumina content increase could be due to the presence of greater amounts of kaolinite.

The correlation of hydroxyl loss with alumina content (Figure 3) is a more clear evidence. Higher alumina contents (higher kaolinite contents) correspond to more hydroxyls in the structure. In fact, kaolinite has more hydroxyls in its lattice than montmorillonite. The ideal hydroxyl weight percentage for a montmorillonite is ~5%. The values lower than 5% shown in Figure 3 are probably due to the presence of oxide anions in hydroxyl positions, as Schultz (1969) proposed. The fact that montmorillonite can have varying hydroxyl amounts may introduce some scattering in the Figure 3 plot.

The Greene-Kelly test did not identify the presence of beidellite in any sample. On the other hand, the diffractograms of the glycolated samples present an important evidence of the presence of kaolinite randomly

interstratified with montmorillonite. The results of 001/002 and 002/005 maxima position analysis have been already shown. But further evidence can be obtained if these results are compared with chemical data. Figure 9 is a plot of $SiO_2:Al_2O_3$ weight % ratios versus kaolinite percentage in a hypothetical kaolinite/montmorillonite mixed-layer. The line unites the $SiO_2:Al_2O_3$ ratios for 0 and 100% kaolinite, and so every intermediate composition must be on it. The $SiO_2:Al_2O_3$ ratio for kaolinite is unique, but not for montmorillonite. The ratio for montmorillonite was taken from the TR-4 sample, which is completely montmorillonitic on the basis of its diffractogram in Figure 5 and the lack of the kaolinite dehydroxylation peak in its DTA diagram. The use of Figure 9 plot to determine kaolinite percentages needs the assumption of that smectite composition remains constant, which is likely to occur. Table 2 shows the agreement between kaolinite percentages obtained by $SiO_2:Al_2O_3$ ratio and by XRD.

NMR results (Figure 8, compare with Table 1) show that tetrahedral Al increases as alumina content decreases. This is expected if the higher amounts of alumina are due to the presence of kaolinite, because there is always some tetrahedral substitution in montmorillonite, but not in kaolinite. Also, this is in agreement with DTA data too (see $\%M_{DTA}$ in Figure 8). Increasing $\%M_{DTA}$ correspond to decreasing amounts of kaolinite, and so to increasing tetrahedral Al.

Notice that these results from NMR definitively rule out the interpretation of these samples as being a montmorillonite-beidellite series, because increasing alumina content would yield increasing tetrahedral Al, which is the opposite of what actually occurs.

CONCLUSIONS

The kaolinite/montmorillonite mixed-layer series are chemically identical to beidellite-montmorillonite ones. For this reason chemical analysis can be deceptive. On the other hand, some beidellites presented in the literature have double dehydroxylation peaks (one in the range 500°–600°C and one in the range 600°–700°C), hydroxyl contents higher than the ideal, or do not respond positively to the Greene-Kelly test. All these features were present in our kaolinite/montmorillonite interstratificates. For this reason several different techniques should be used to assure the beidellitic character of a smectitic material.

ACKNOWLEDGMENTS

Table 2. Comparison of kaolinite percentages in the mixed-layer obtained from diffractograms and $SiO_2:Al_2O_3$ ratios. LT-10/6 sample showed an intermediate percentage in the XRD determination.

Sample	% Kaolinite	
	$SiO_2:Al_2O_3$ method	XRD
T-20	17.3	20
LT-2	39.5	40
LT-9/3	13.0	10
LT-10/1	36.4	40
LT-10/6	16.0	10 < k < 20
TR-4	0.0	0
TR-117	32.1	40
TR-119	17.3	10
TR-121	24.1	30

REFERENCES

Borchardt, G. A. (1977) Montmorillonite and other smectite minerals: in *Minerals in Soil Environments,* J. B. Dixon and S. B. Weed, eds., Soil Sci. Soc. Amer., Madison, Wisconsin, 293–330.

Brindley, G. W. and Lemaitre, J. (1987) Thermal oxidation and reduction reactions of clay minerals: in *Chemistry of Clays and Clay Minerals,* A. C. D. Newman, ed., Longman Scientific and Technical (Essex), Mineralogical Society, London, 319–370.

Bystrom-Brusewitz, A. M. (1975) Studies of the Li-test to distinguish beidellite and montmorillonite: in *Proceedings of the International Clay Conference, 1975,* Applied Publishing Ltd., Wilmette, Illinois, 419–428.

Farmer, V. C. (1974) The layer silicates: in *The Infrared Spectra of Minerals,* V. C. Farmer, ed., Mineralogical Society, London, 331–364.

Greene-Kelly, R. (1952) A test for montmorillonite: *Nature,* **170**: 1130.

Güven, N. (1991) Smectites: in *Hydrous Phyllosilicates,* S. W. Bailey, ed., Reviews in Mineralogy, Vol. 19, Chelsea, 497–560.

Mackenzie, R. C. (1970) Simple phyllosilicates based on gibbsite- and brucite-like sheets: in *Differential Thermal Analysis, Vol. 1,* R. C. Mackenzie, ed., Academic Press, New York, 504–511.

Malla, P. B. and Douglas, L. A. (1987) Layer charge properties of smectites and vermiculites: Tetrahedral vs. octahedral: *Soil Sci. Soc. Amer. J.,* **51**: 1362–1366.

Marshall, C. E. (1949) The structural interpretation of chemical analyses of the clay minerals: in *The Colloid Chemistry of the Silicate Minerals,* Academic Press, New York, 56–66.

Moore, D. M. and Reynolds, R. C. Jr. (1989) *X-Ray Diffraction and the Identification and Analysis of Clay Minerals:* Oxford University Press, Oxford, New York.

Newman, A. C. D. and Brown, G. (1987) The chemical constitution of clays: in *Chemistry of Clays and Clay Minerals,* A. C. D. Newman, ed., Longman Scientific and Technical (Essex), Mineralogical Society, London, 1–128.

Paterson, E. and Swaffield, R. (1987) Thermal analysis: in *A Handbook of Determinative Methods in Clay Mineralogy,* M. J. Wilson, ed., Chapman and Hall, New York, 99–132.

Reyes, E., Huertas, F. and Linares, J. (1978) [Génesis y geoquímica de las esmectitas de Andalucía (España)]. Genesis and geochemistry of the smectites of Andalucía (Spain): *Proceedings of 1st International Congress on Bentonites, Sassari-Calgari, 1978,* 149–176.

Russel, J. D. (1987) Infrared methods: in *A Handbook of Determinative Methods in Clay Mineralogy,* M. J. Wilson, ed., Chapman and Hall, New York, 133–173.

Schultz, L. G. (1969) Lithium and potassium absorption, dehydroxylation temperature, and structural water content of aluminous smectites: *Clays and Clay Minerals,* **17**: 115–149.

SCIFAX DTA Data Index (1962) Compiled by R. C. Mackenzie, Cleaver-Hume Press, London.

Soil Conservation Service (1972) *Soil Survey Laboratory Methods and Procedure for Collecting Soil Samples,* U.S.D.A., Washington, D.C., Method 5A6.

Wilson, M. J. (1987) X-ray powder diffraction methods: in *A Handbook of Determinative Methods in Clay Mineralogy,* M. J. Wilson, ed., Blackie, London, 26–98.